

Received March 24, 2020, accepted April 12, 2020, date of publication April 20, 2020, date of current version May 5, 2020.

Digital Object Identifier 10.1109/ACCESS.2020.2988789

Study on the Verification of the Calculated Harmonic Impedance

FANGWEI XU¹, (Member, IEEE), WEI PU¹, JINSHUAI ZHAO¹, (Student Member, IEEE), ZHIQUAN MA², AND WENTAO LV²

¹School of Electrical Engineering, Sichuan University, Chengdu 610065, China

²State Grid Zhejiang Electric Power Research Institute, Hangzhou 310014, China

Corresponding author: Jinshuai Zhao (jinshuai_zhao_scu@163.com)

This work was supported in part by the National Natural Science Foundation of China under Grant 51877141 and Grant 51842703.

ABSTRACT The verifications of the calculated harmonic impedances are necessary for harmonic impedance estimation. Among the existing methods of the verifications, the method, by matching the calculated background harmonic voltage with the measured voltage when the customer is out of operation, is widely used. The background harmonics can be calculated based on IEC61000-3-6 (named as the IEC method) or the superposition index. However, some researchers ignore the fact that these two methods cannot be chosen arbitrarily, otherwise, the misjudgments may occur. In our study, the nonlinear customers are classified into two categories according to the ways how they are out of operation: 1) only the harmonic source is cut off, and 2) the harmonic source and the impedance of the customer side are both cut off. Then, the differences in using the IEC method and the superposition index to match the calculated and measured background harmonic voltage are investigated. Finally, based on the properties of the two methods and the categories of the customers, a framework is proposed to accurately validate the calculated harmonic impedance. The effectiveness and reliability of the proposed framework are verified through simulation and field case studies.

INDEX TERMS Background harmonic voltage, harmonic impedance, impedance verification, IEC61000-3-6, superposition index.

I. INTRODUCTION

With the development of power electronic devices and the increase of nonlinear loads, harmonic pollution in power system becomes more and more serious [1]–[4]. Harmonics increase power losses and reduce the service life of the components in power grid such as transformers and transmission lines, and ultimately reduce the operating efficiency of the power system. More seriously, harmonics lead to series or parallel resonance, electromagnetic interference, and the maloperation at the protections [2], destroying the stable operation of the power system. To solve the harmonic issue, the researchers have conducted a series of harmonic studies on power systems. One of the most indispensable studies is about the harmonic impedance (shown in figure 1), which can be divided into three parts: 1) calculation of the harmonic impedance; 2) validation of the calculated impedance; and

3) application of the calculated harmonic impedance. For part 1), many noninvasive methods have been proposed for harmonic impedance estimation based on the harmonic measurements at a point of common coupling (PCC) [5]–[13]. Meanwhile, part 3) has been extensively studied, such as calculation of the harmonic contributions, harmonic control, and design of filter, etc. [14]–[17]. In comparison, related study for part 2) is a gap. Yet, the validation of the calculated result is still significant, because only the correct result can be applied in part 3). Therefore, to consummate part 2), a framework is proposed to validate the calculated harmonic impedance.

In reference [5], the actual harmonic impedance can be roughly calculated according to the known grid structure and the parameters of its main components, but the structure and parameters are difficult to obtain. In reference [6]–[8], [17] the harmonic impedance of the last transformer before the connection point is regarded as the reference value of the utility harmonic impedance. Yet, this method is applicable

The associate editor coordinating the review of this manuscript and approving it for publication was Firuz Zare.

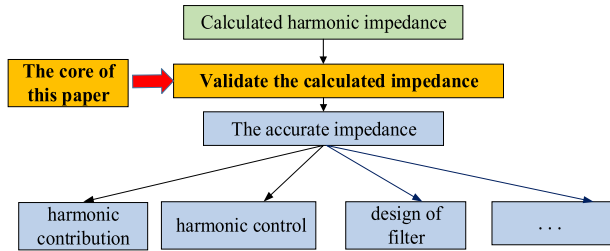


FIGURE 1. Harmonic impedance studies on power systems.

only when the utility side is inductive. In reference [9]–[11], [18], the reference impedance is obtained by the ratio of the harmonic voltage difference to the current difference at the PCC before and after the customer manually switching off. However, this method can only verify the utility harmonic impedance, but not the customer impedance. In reference [11]–[13], the voltage measured at the PCC when the customer is out of operation is regarded as the reference voltage, and then the calculated background harmonic voltage is matched with it. Comparing with the above methods, this method can verify the harmonic impedance of both sides and be applied more extensively.

As mentioned in [11]–[13], after obtaining the harmonic impedance, the background harmonic voltage can be calculated and matched with the measured background harmonic voltage, so as to verify whether the calculated harmonic impedance is correct. Generally, the background harmonic voltage can be calculated based on the IEC method [9]–[12] or the superposition index [13], [19]–[21]. However, the researchers do not distinguish the difference of the both methods in terms of application situations. In this paper, finding that these two methods cannot be chosen arbitrarily, otherwise, some misjudgments may occur. According to the ways how nonlinear customers are out of operation, the harmonic customers are classified into two categories: 1) the harmonic source and the impedance of the customer side are both cut off, such as arc furnace, and 2) only the harmonic source is cut off, such as wind farm and photovoltaic farm (see Figure 2). For the category 1 (defined as model A in Figure 2), the measured background harmonic voltage should only be matched with the calculated values based on the IEC method instead of the superposition index. For the category 2 (defined as model B in Figure 2), the measured background harmonic voltage should only be matched with the calculated values based on the superposition index instead of the IEC method. In a word, model A should be matched with the IEC method, and model B should be matched with the superposition index, whose reason is explained in detail in Section II.

Note that, if the matching is chosen wrong, the validity of the harmonic impedance estimation will be misjudged. For example, in reference [11], [12], where the nonlinear customer is just arc furnace, the IEC method is used to validate the calculated harmonic impedance. However, if the

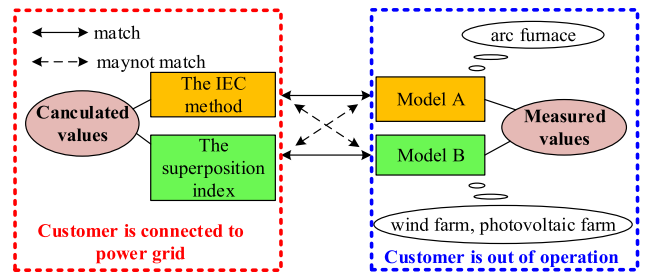


FIGURE 2. Matching diagram.

arc furnace is replaced by the customer belonging to model B, the validity of the calculated impedance will be misjudged. Besides, the similar problem also exists in reference [13] for the analysis of the 7th harmonic.

In order to accurately verify the validity of the calculated harmonic impedances, a framework is proposed in this paper. First, the nonlinear customers are classified into two categories (i.e. model A and model B) based on the way how they are out of operation. Then, the differences and commonness between the IEC method and the superposition index in terms of application situations are analyzed. Finally, according to the category of the customer, the method of calculating the background harmonic voltage is selected to validate the harmonic impedance. The effectiveness and reliability of the proposed framework are demonstrated by simulations and multiple field cases.

This paper is organized as follows. Section II presents the principle and framework of validating the harmonic impedance. Section III and IV demonstrates the effectiveness of the proposed framework through simulation and field cases. Section V concludes.

II. VALIDATION OF THE CALCULATED HARMONIC IMPEDANCE

In practical engineering, the validity of the calculated harmonic impedances can be indirectly verified by matching the calculated background harmonic voltage with the voltage measured when the customer is out of operation. Generally, there are two methods to calculate the background harmonics: the IEC method and the superposition index. The differences in using the two methods to match the calculated and measured values are investigated below.

A. CALCULATION OF THE BACKGROUND HARMONIC VOLTAGE BASED ON THE IEC METHOD

In the Norton circuit corresponding to the IEC method (Figure 3), Z_u , Z_c and \dot{I}_u , \dot{I}_c are the harmonic impedances and currents of the utility and the customer sides respectively, while \dot{V}_{pcc} and \dot{I}_{pcc} are the harmonic voltage and current measured at the PCC.

When the switch is closed, the customer is connected to the power grid, and the harmonic voltage at the PCC is

$$\dot{V}_{pcc\text{-post}} = \dot{I}_u Z_u + \dot{I}_{pcc} Z_u \quad (1)$$

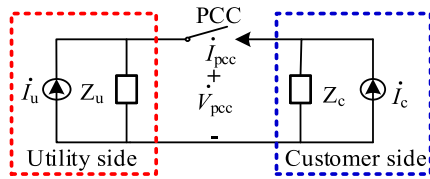


FIGURE 3. Norton equivalent circuit of the IEC method.

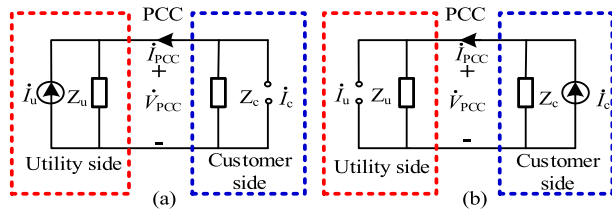


FIGURE 4. Norton circuit related to the superposition index. (a) Harmonic emission level of the utility side. (b) Harmonic emission level of the customer side.

When the switch is off, the customer side is out of operation, and the harmonic voltage at the PCC is

$$\dot{V}_{pcc-pre} = \dot{I}_u Z_u \quad (2)$$

According to the standard IEC61000-3-6 [22], the harmonic voltage emission level of a customer is the difference of the harmonic voltage before and after the customer being connected to the network [11], [23]. Referring to this standard, the harmonic emission levels of the customer and the utility sides can be respectively expressed as

$$\dot{V}_{c-pcc}^{IEC} = \dot{I}_{pcc} Z_u \quad (3)$$

$$\dot{V}_{u-pcc}^{IEC} = \dot{I}_u Z_u. \quad (4)$$

B. CALCULATION OF THE BACKGROUND HARMONIC VOLTAGE BASED ON THE SUPERPOSITION INDEX

Figure 4 is the Norton circuit related to the superposition index. When \dot{I}_u or \dot{I}_c work alone, the corresponding harmonic voltage at the PCC are the harmonic voltage emission level of each source, expressed respectively as

$$\dot{V}_{u-pcc}^{sup} = \frac{Z_c Z_u}{Z_c + Z_u} \dot{I}_u, \quad (5)$$

$$\dot{V}_{c-pcc}^{sup} = \frac{Z_c Z_u}{Z_c + Z_u} \dot{I}_c \quad (6)$$

C. A FRAMEWORK TO VERIFY THE VALIDITY OF THE CALCULATED HARMONIC IMPEDANCE

While the nonlinear customers are connected to the power grid, if Z_u and Z_c are estimated accurately, the calculated background harmonic voltage is also accurate. The validity of the calculated harmonic impedances can be verified indirectly with this principle. When the nonlinear customers are out of operation, the harmonic voltage measured at the PCC is regarded as the reference voltage. Therefore, by matching the calculated voltage with the reference voltage, the correctness of the calculated Z_u and Z_c can be verified.

In practice, the nonlinear customers are diverse and complex. In this paper, they are classified into two categories as follows according to the way how they are out of operation.

- **Model A:**

For nonlinear customers such as arc furnace, both the harmonic source and the harmonic impedance are cut off when the customers are out of operation. For this kind of customers, the background harmonic voltage should be calculated based on the circuit model of the IEC method. The reference voltage is defined as \dot{V}_{u-pcc}^A which can be theoretically calculated using Eq. (4) by replacing \dot{V}_{u-pcc}^{IEC} with \dot{V}_{u-pcc}^A . Therefore, when Z_u is calculated accurately, \dot{V}_{u-pcc}^{IEC} is equal to \dot{V}_{u-pcc}^A . Notably, since there isn't Z_c in Eq. (4), this method cannot judge the correctness of the calculated Z_c .

- **Model B:**

For nonlinear customers such as wind farms, photovoltaic farms, etc., when the customers are out of operation, the harmonic source is cut off, while the harmonic impedance is still connected to the power grid. For this kind of customers, the background harmonic voltage should be calculated based on the model of superposition index. The reference voltage is defined as \dot{V}_{u-pcc}^B which can be theoretically calculated using Eq. (5) by replacing \dot{V}_{u-pcc}^{sup} with \dot{V}_{u-pcc}^B . Therefore, when both Z_u and Z_c are calculated accurately, \dot{V}_{u-pcc}^{sup} is equal to \dot{V}_{u-pcc}^B . Note that, since Eq. (5) is related to both Z_u and Z_c , \dot{V}_{u-pcc}^{sup} equaling to \dot{V}_{u-pcc}^B can verify the correctness of the calculated impedances for the both sides.

After determining the customer category, the calculated harmonic impedance can be validated based on the amplitude relationship between Z_c and Z_u . The detailed processes are described as follows.

1) $|Z_c|$ IS NOT MUCH LARGER THAN $|Z_u|$

In engineering practice, $|Z_c|$ is not much larger than $|Z_u|$ means that $|Z_c|$ will not exceed ten times of $|Z_u|$. When $|Z_c|$ is not much larger than $|Z_u|$, according to Eqs. (4) and (5), obviously, the calculated background harmonic voltage \dot{V}_{u-pcc}^{IEC} and \dot{V}_{u-pcc}^{sup} are not equaling to each other. Therefore, \dot{V}_{u-pcc}^{IEC} is not equal to \dot{V}_{u-pcc}^B , and \dot{V}_{u-pcc}^{sup} is not equal to \dot{V}_{u-pcc}^A . Theoretically, for model A, the background harmonic voltage calculated by the superposition index can't be matched with the voltage measured after the customer is cut off. Similarly, for model B, the background harmonic voltage calculated by the IEC method can't be matched with the measured voltage. Consequently, if the method of calculating the background harmonic voltage (i.e., the IEC method or superposition index) is chosen wrong, the calculated harmonic impedance will be misjudged as wrong, even when the calculation result is accurate.

To avoid the above misjudgment, the customer model must be matched with the correct method (the IEC method or the superposition index).

2) $|Z_c|$ IS MUCH LARGER THAN $|Z_u|$

Under this situation, the calculation errors of Z_c are usually unacceptable [10], [13]. Thus, only the accuracy of the calculated Z_u should be verified. Since $|Z_c| \gg |Z_u|$, then $Z_u/Z_c \approx 0$, and Eq. (5) can be transformed into Eq. (7). Hence, the background harmonic voltage can be calculated by the superposition index without Z_c .

$$\dot{V}_{u-pcc}^{sup} = \frac{Z_u}{1 + Z_u/Z_c} \dot{I}_u \approx Z_u \dot{I}_u. \quad (7)$$

Note that, at this moment, Eq. (7) is equivalent to Eq. (4), and the calculated \dot{V}_{u-pcc}^{IEC} and \dot{V}_{u-pcc}^{sup} are approximately equal to each other. Thus, the calculated Z_u can be validated based on either the IEC method or the superposition index no matter what model the customer is.

3) DETERMINATION THE RELATIONSHIP OF $|Z_c|$ AND $|Z_u|$

When $|Z_c| \gg |Z_u|$, $Z_u/Z_c \approx 0$, \dot{I}_{pcc} can be represented as

$$\dot{I}_{pcc} = \frac{Z_c}{Z_c + Z_u} \dot{I}_c - \frac{Z_u}{Z_c + Z_u} \dot{I}_u \approx \dot{I}_c. \quad (8)$$

Therefore, by evaluating the similarity between \dot{I}_{pcc} and \dot{I}_c , whether $|Z_c| \gg |Z_u|$ holds can be indirectly determined. In this evaluation process, the source signal \dot{I}_c can be recovered by the independent component analysis (ICA) algorithm [13]. The ICA is a blind source separation technique which extract original signals from the observed signals without knowing how the source signals mixed.

According to the Norton equivalent circuit (Figure 3 or Figure 4), we have

$$\underbrace{\begin{bmatrix} \dot{V}_{pcc} \\ \dot{I}_{pcc} \end{bmatrix}}_X = \underbrace{\begin{bmatrix} \frac{Z_c Z_u}{Z_c + Z_u} & \frac{Z_c Z_u}{Z_c + Z_u} \\ \frac{Z_c}{Z_c + Z_u} & -\frac{Z_u}{Z_c + Z_u} \end{bmatrix}}_Z \underbrace{\begin{bmatrix} \dot{I}_c \\ \dot{I}_u \end{bmatrix}}_I \quad (9)$$

where matrix X contains the observed signals \dot{V}_{pcc} and \dot{I}_{pcc} , matrix I contains the source signals \dot{I}_u and \dot{I}_c , and matrix Z is a mixed impedance matrix. Before using the ICA algorithm, the fast-varying components of matrix X (\dot{V}_{pcc}^{fast} and \dot{I}_{pcc}^{fast}) need to be extracted respectively by using the linear filter [13]. Then, \dot{V}_{pcc}^{fast} and \dot{I}_{pcc}^{fast} can be applied to recover the fast-varying components of the source signals \dot{I}_u^{fast} and \dot{I}_c^{fast} though the ICA algorithm. After that, the estimated impedance matrix \hat{Z} can be calculated by

$$\hat{Z} = X \hat{I}^T (\hat{I} \hat{I}^T)^{-1} \quad (10)$$

where \hat{I} is the source signal recovered by the ICA algorithm. However, ordering and scaling indeterminacies are in the

above process as shown in Eqs. (11) and (12) [10].

$$\underbrace{\begin{bmatrix} \dot{V}_{pcc}^{fast} \\ \dot{I}_{pcc}^{fast} \end{bmatrix}}_X = \underbrace{\begin{bmatrix} w_1 \frac{Z_c Z_u}{Z_c + Z_u} & w_2 \frac{Z_c Z_u}{Z_c + Z_u} \\ w_1 \frac{Z_c}{Z_c + Z_u} & -w_2 \frac{Z_u}{Z_c + Z_u} \end{bmatrix}}_{\hat{Z}} \underbrace{\begin{bmatrix} \frac{1}{w_1} \hat{I}_c^{fast} \\ \frac{1}{w_2} \hat{I}_u^{fast} \end{bmatrix}}_{\hat{I}}, \quad (11)$$

$$\underbrace{\begin{bmatrix} \dot{V}_{pcc}^{fast} \\ \dot{I}_{pcc}^{fast} \end{bmatrix}}_X = \underbrace{\begin{bmatrix} w_2 \frac{Z_c Z_u}{Z_c + Z_u} & w_1 \frac{Z_c Z_u}{Z_c + Z_u} \\ -w_2 \frac{Z_u}{Z_c + Z_u} & w_1 \frac{Z_c}{Z_c + Z_u} \end{bmatrix}}_{\hat{Z}} \underbrace{\begin{bmatrix} \frac{1}{w_2} \hat{I}_u^{fast} \\ \frac{1}{w_1} \hat{I}_c^{fast} \end{bmatrix}}_{\hat{I}}, \quad (12)$$

where w_1 and w_2 are uncertain coefficients that represent scaling indeterminacy. Obviously, the order in matrix \hat{I} is uncertain, which named ordering indeterminacies. To overcome these two indeterminacies, define

$$\begin{cases} k_1 = \hat{Z}(1, 1)/\hat{Z}(2, 1) \\ k_2 = \hat{Z}(1, 2)/\hat{Z}(2, 2) \end{cases} \quad (13)$$

Since the real part of the impedance in power system is always positive, the order can be determined though the sign of $R(k_1)$ and $R(k_2)$ where R means the real part. If $R(k_1) > 0$ and $R(k_2) < 0$, as the case with Eq. (11), $Z_u = k_1$ and $Z_c = -k_2$. Otherwise, in the case of Eq. (12), $Z_c = -k_1$ and $Z_u = -k_2$. After estimating Z_u and Z_c , \hat{I}_c^{fast} can be estimated. Furthermore, the similarity between \dot{I}_{pcc}^{fast} and \hat{I}_c^{fast} can be calculated by the correlation coefficient expressed in Eq. (14). The larger the correlation coefficient is, the higher the similarity is. Empirically, when σ in Eq. (14) is larger than 0.9, it can be considered that $|Z_c|$ is much larger than $|Z_u|$.

$$\sigma(X, Y) = \frac{\text{Cov}(X, Y)}{\sqrt{\text{Var}[X] \text{Var}[Y]}}. \quad (14)$$

where X and Y correspond to the amplitudes of \dot{I}_{pcc}^{fast} and \hat{I}_c^{fast} , respectively; $\text{Cov}(X, Y)$ is the covariance of X and Y ; $\text{Var}[X]$ and $\text{Var}[Y]$ are the variance of X and Y , respectively.

The flow chart of the proposed framework above is presented in Figure 5.

III. SIMULATION STUDY

The circuit models shown in Figure 3 and Figure 4 (a) are utilized to simulate model A and model B, respectively. The simulation analysis of the two models is based on two cases: 1) $|Z_c|$ is not much larger than $|Z_u|$, and 2) $|Z_c| \gg |Z_u|$. The harmonic currents and impedances are set as follows.

Harmonic current sources: The amplitude and phase angle of \dot{I}_u are respectively set as 150 A and 50° . The amplitude and phase angle of \dot{I}_c are respectively set as 150 A and -35° . 50% sinusoidal fluctuations and $\pm 5\%$ random disturbances are added to the amplitude and phase angle of both \dot{I}_u and \dot{I}_c .

The parameters of impedances are shown in Table 1.

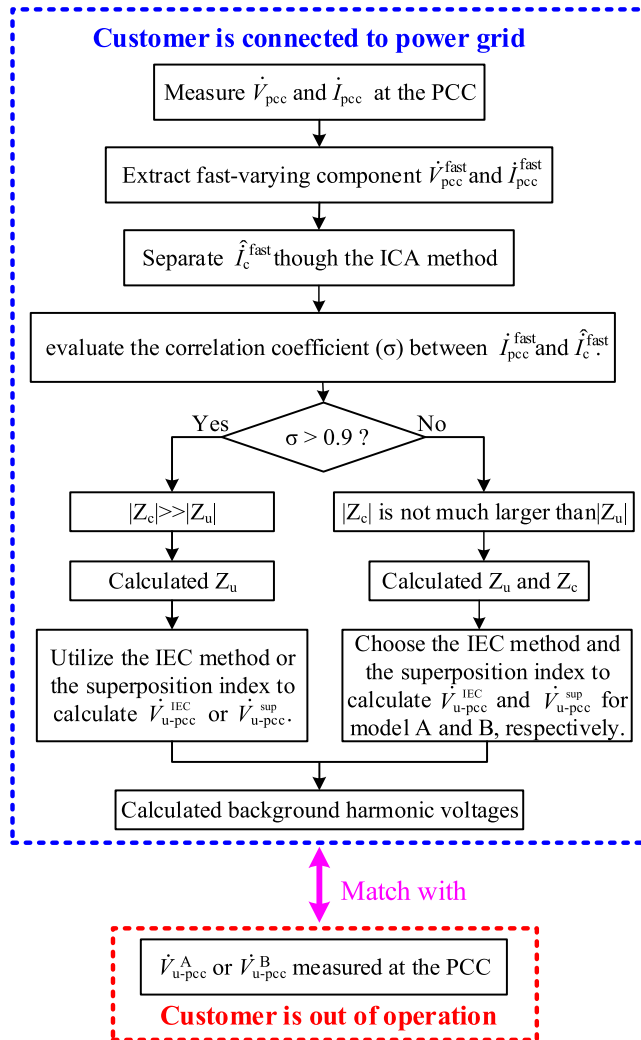


FIGURE 5. The flow chart of the harmonic impedance validity verification.

TABLE 1. Simulation parameters.

$ Z_c $ is not much large than $ Z_u $		$ Z_c \gg Z_u $	
Z_u (Ω)	Z_c (Ω)	Z_u (Ω)	Z_c (Ω)
$1+j8$	$2+j10$	$1+j8$	$15+j100$

On the basis of the above harmonic currents and impedances, 3000 PCC data are generated for the analysis of the impedance calculation. Although various of the calculation methods have been proposed, most of them can only calculate Z_u . In comparison, the ICA method can estimate both Z_u and Z_c [6], [10], [12], [13]. Therefore, the proposed framework is used to validate the harmonic impedances calculated by ICA.

A. $|Z_c|$ IS NOT MUCH LARGER THAN $|Z_u|$

In this situation, the harmonic impedances calculated by ICA are shown in Table 2. It can be concluded that both Z_u and Z_c are estimated accurately. By referring to this conclusion, the validity of our proposed framework can be verified.

TABLE 2. Calculated results.

Impedance	Calculation (Ω)	Amplitude error (%)	Phase error (%)
Z_u	$1.0046 + j7.7360$	3.24	0.33
Z_c	$2.0770 + j9.8772$	1.03	0.72

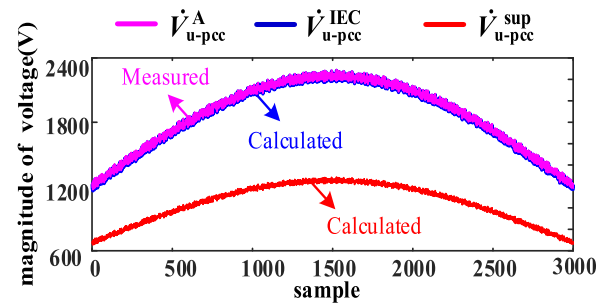


FIGURE 6. Calculated and measured background harmonic voltages.

The customers are classified into two categories in the following verification analysis.

1) THE CUSTOMER BELONGS TO MODEL A

According to the proposed framework, the IEC method should be chosen to calculate the background harmonic voltages in this case. The simulation results are shown in Figure 6. Obviously, the calculation results of the IEC method ($|\dot{V}_{u-pcc}^{IEC}|$) are consistent with the measured background harmonics ($|\dot{V}_{u-pcc}^A|$), which correctly validate the calculated Z_u . In contrast, if the superposition index is chosen, huge differences exist between the calculation results ($|\dot{V}_{u-pcc}^{sup}|$) and $|\dot{V}_{u-pcc}^A|$. Thus, wrongly conclusion will be drawn that the calculated Z_u are with large errors. Notably, the correctness of the calculated Z_c cannot be determined in model A as is analyzed in Section II.

2) THE CUSTOMER BELONGS TO MODEL B

In this case, the superposition index should be chosen to estimate the background harmonic voltages. Figure 7 indicates that the calculation results ($|\dot{V}_{u-pcc}^{sup}|$) are coincided with the measured background harmonics ($|\dot{V}_{u-pcc}^B|$). Therefore, it can be concluded that both Z_u and Z_c are calculated correctly. In comparison, the estimated curve of the IEC method ($|\dot{V}_{u-pcc}^{IEC}|$) has huge differences with $|\dot{V}_{u-pcc}^B|$. Thus, misjudgment will be drawn that Z_u and Z_c are calculated wrongly.

B. $|Z_c|$ IS MUCH LARGER THAN $|Z_u|$

In this condition, the calculation errors of Z_c is generally wrong; thus, there is no need to validate its correctness. Two categories of customers are considered (Figure 8 and Figure 9). For each case, $|\dot{V}_{u-pcc}^{IEC}|$ and $|\dot{V}_{u-pcc}^{sup}|$ calculated by the IEC method and the superposition index are close to the harmonic voltages measured when the customer is out of operation. Thus, it can be concluded that Z_u is accurately estimated. Furthermore, Table 3 also indicates that the errors

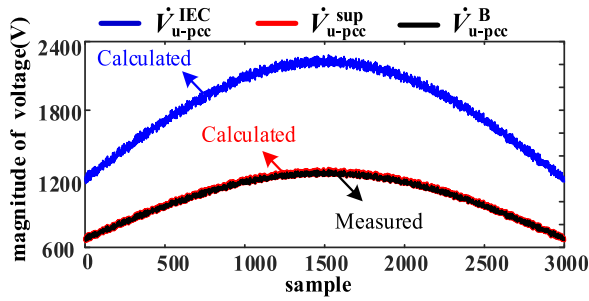


FIGURE 7. Calculated and measured background harmonic voltages.

TABLE 3. Calculated results.

Impedance	Calculation (Ω)	Amplitude error (%)	Phase error (%)
Z_u	$0.9447+j7.7592$	3.05	0.22
Z_c	$14.713+125.35$	24.81	2.25

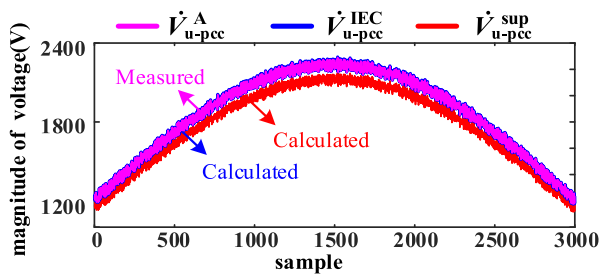


FIGURE 8. Calculated and measured background harmonic voltages.

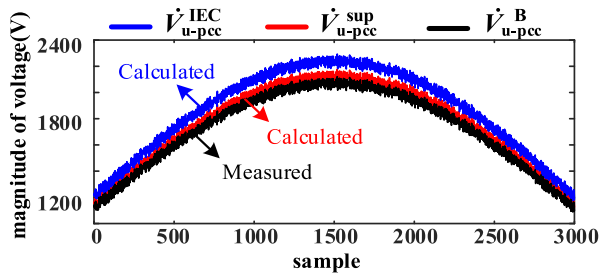


FIGURE 9. Calculated and measured background harmonic voltages.

of Z_u are extremely low. Consequently, the conclusions of our proposed framework are correct.

IV. FIELD TEST VERIFICATION

A. CASE 1: MODEL A

Arc furnace, as a typical customer in model A, is used to verify the practicability of the proposed framework in this section. The data is measured from a 150kV bus of 100 MW DC arc furnace, with sampling frequency of 6400 Hz. Harmonics with respect to each harmonic order are obtained by utilizing Fast Fourier transform to analyze the voltage and current simple data per minute.

Generally, two single-tuned filters are installed at the customer side to mitigate the 5th and 7th harmonics, which may cause $|Z_c|$ is not much larger than $|Z_u|$. Besides, for

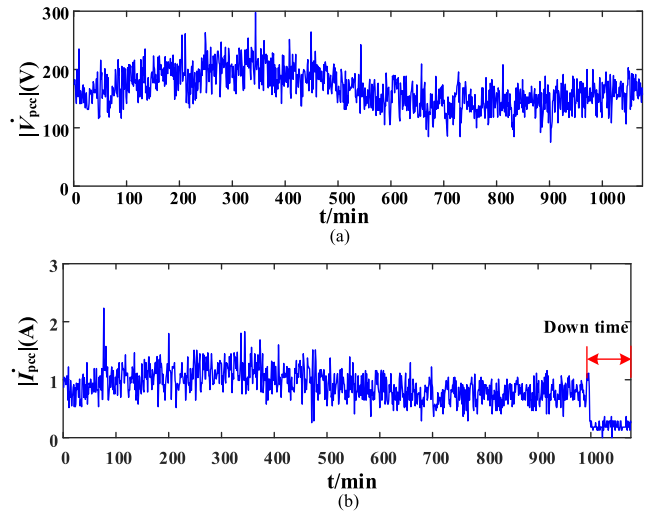


FIGURE 10. The 5th harmonic voltages and currents measured at the PCC. (a) The 5th harmonic voltages. (b) The 5th harmonic currents.

other harmonic orders, e.g., 3rd harmonics, usually meet $|Z_c| \gg |Z_u|$. To comprehensively validate our proposed framework, the situations for 3rd and 5th harmonics are discussed as follows.

1) THE 5TH HARMONICS

The 5th harmonic voltages and currents are shown in Figure 10. After 1000 minutes, the arc furnace is out of operation for a short period (corresponding to the down time).

Based on the harmonic impedances estimated from the ICA method, the calculated background harmonics and the separated \hat{I}_c^{fast} are shown in Figure 11. Obvious differences exist between the extracted \hat{I}_{pcc}^{fast} and the estimated \hat{I}_c^{fast} . Meanwhile, the correlation coefficient between \hat{I}_{pcc}^{fast} and \hat{I}_c^{fast} (calculated as 0.330) is relatively low. Thus, it can be determined that $|Z_c|$ is not much larger than $|Z_u|$. Referring to our proposed framework, $|\hat{V}_{u-pcc}^A|$ should be matched with $|\hat{V}_{u-pcc}^{IEC}|$ instead of $|\hat{V}_{u-pcc}^{sup}|$. Figure 11 (b) represents that $|\hat{V}_{u-pcc}^A|$ is matched with $|\hat{V}_{u-pcc}^{IEC}|$, which validates the calculated Z_u . In comparison, great differences exist between $|\hat{V}_{u-pcc}^A|$ and $|\hat{V}_{u-pcc}^{sup}|$. Thus, if the superposition index is chosen to calculate the background harmonic voltages, misjudgment will be drawn that Z_u is calculated wrongly.

To further verify the above judgements, the probability density diagrams of the background harmonic voltages are shown in Figure 12. The probability density curve of $|\hat{V}_{u-pcc}^{IEC}|$ is close to $|\hat{V}_{u-pcc}^A|$, while the difference between $|\hat{V}_{u-pcc}^{sup}|$ and $|\hat{V}_{u-pcc}^A|$ is large, hence the validity of the conclusions from our proposed framework are further verified.

2) THE 3RD HARMONICS

The 3rd harmonics shown in Figure 13 are used to verify the effectiveness of our proposed framework when $|Z_c| \gg |Z_u|$.

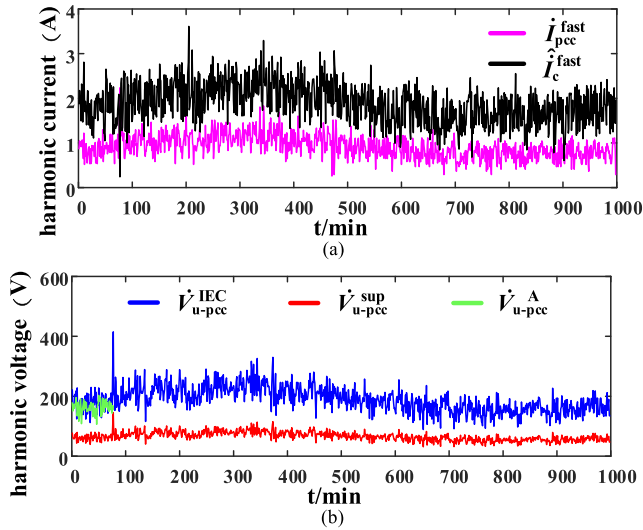


FIGURE 11. The 5th harmonic waveforms of the photovoltaic farm. (a) Extracted j_{pcc}^{fast} and estimated j_c^{fast} . (b) Calculated and measured background harmonics.

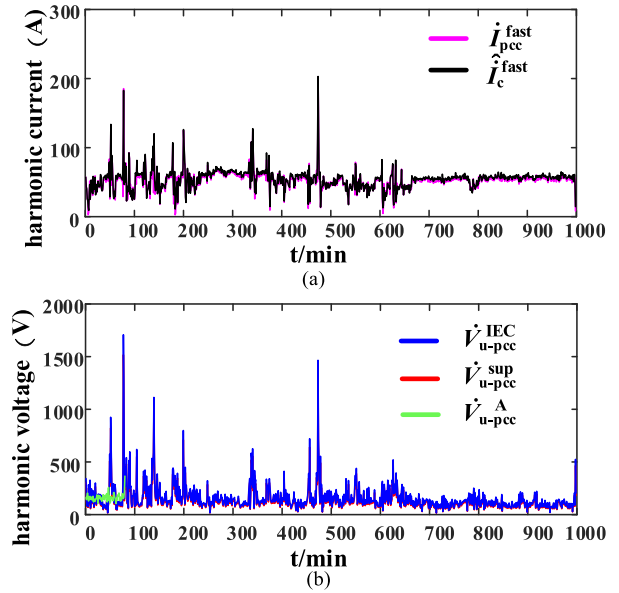


FIGURE 14. The 3rd harmonic waveforms of the photovoltaic farm. (a) Extracted j_{pcc}^{fast} and estimated j_c^{fast} . (b) Calculated and measured background harmonics.

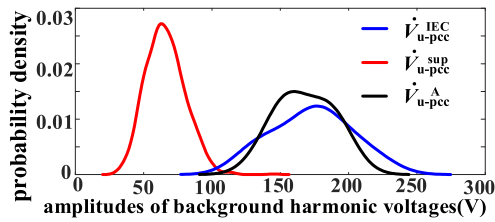


FIGURE 12. Probability density of background harmonic voltages.

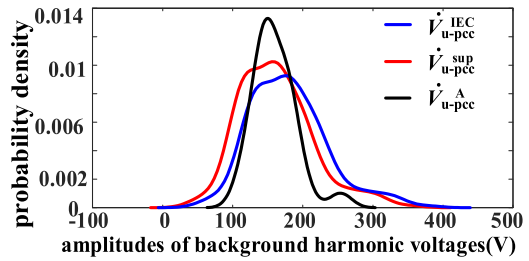


FIGURE 15. Probability density of background harmonic voltages.

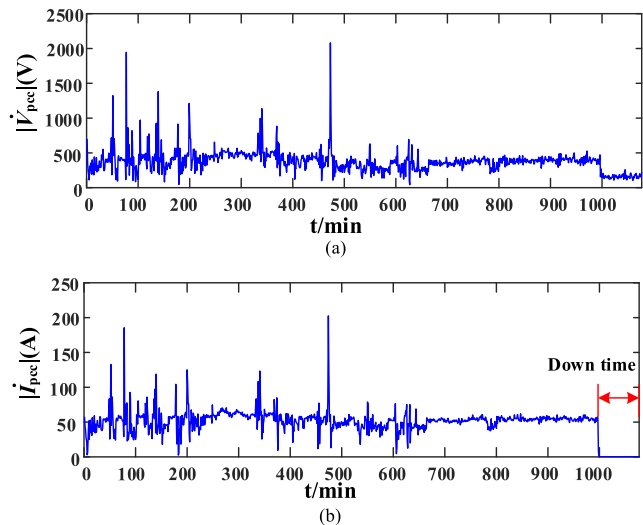


FIGURE 13. The 3rd harmonic voltages and currents measured at the PCC. (a) The 3rd harmonic voltages. (b) The 3rd harmonic currents.

Figure 14 (a) shows that the \hat{j}_c^{fast} reconstructed from the ICA is almost coincided with the extracted j_{pcc}^{fast} . Besides, the correlation coefficient between j_{pcc}^{fast} and \hat{j}_c^{fast} (calculated as 0.967) is larger than 0.9. Thus, $|Z_c| \gg |Z_u|$ can be determined. At this condition, theoretically, the background

harmonic voltages estimated from either the IEC method or the superposition index can be used to validate the calculated Z_u . Actually, the calculated background harmonics $|\hat{V}_{u-pcc}^{IEC}|$ and $|\hat{V}_{u-pcc}^{sup}|$ are matched with the measured $|\hat{V}_{u-pcc}^A|$ as shown in Figure 14 (b). Hence, it can be concluded that the calculated Z_u is with high accuracy.

Furthermore, the probability density curves corresponding to $|\hat{V}_{u-pcc}^{IEC}|$ and $|\hat{V}_{u-pcc}^{sup}|$ are just close to that of $|\hat{V}_{u-pcc}^A|$ (Figure 15). Thus, the above conclusions are further validated.

Besides, a customer belonging to model A is also studied in the field test of reference [13]. The harmonic voltages measured when this customer is out of operation are used to validate the calculated harmonic impedance. Based on our proposed framework, the IEC method should be chosen to estimate the background harmonic voltage in the validation process. Although the superposition index is chosen in reference [13], for the 5th harmonic, the calculated Z_u can still be accurately verified since $|Z_c| \gg |Z_u|$. Notably, for the 7th harmonic impedance, since $|Z_c|$ is not much larger than $|Z_u|$, the correctness of the calculated harmonic impedance will be misjudged.

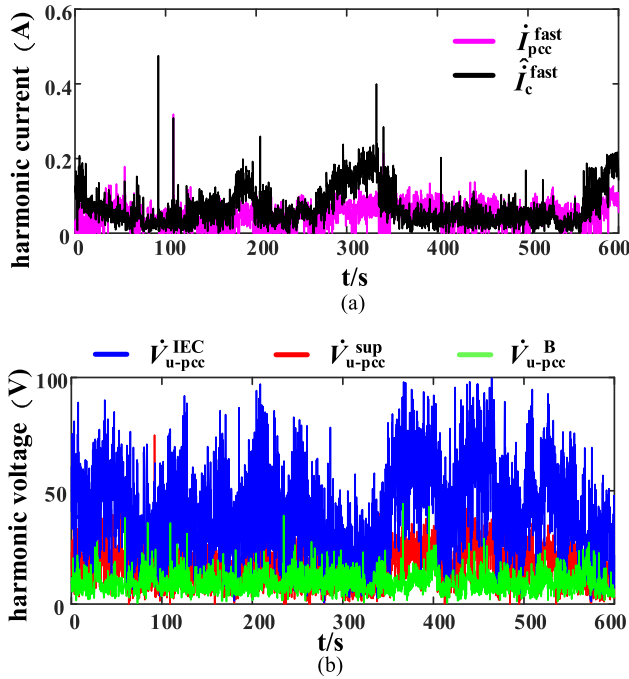


FIGURE 16. The 23rd harmonic waveforms of the photovoltaic farm. (a) Extracted \hat{i}_{pcc}^{fast} and estimated \hat{i}_c^{fast} . (b) Calculated and measured background harmonics.

B. CASE 2: MODEL B

When a photovoltaic farm is out of operation at night, the relative electric components e.g., the transformers, the lines, and the filters, etc., are still connected with the power grid. Thus, only the harmonic source parts are cut off. In this paper, a photovoltaic farm in China is treated as a typical customer for model B to analyze the proposed framework.

Since the harmonic filters are installed in the photovoltaic farm, $|Z_c|$ is not much larger than $|Z_u|$ for some harmonic orders (e.g., the 23th harmonics). Additionally, for other harmonic orders, $|Z_c| \gg |Z_u|$ is satisfied (e.g., the 9th harmonics). Here, to completely validate the proposed framework, both the 23th and the 9th harmonics are analyzed:

1) THE 23RD HARMONICS

It can be determined from Figure 16 (a) that $|Z_c|$ is not much larger than $|Z_u|$ because \hat{i}_{pcc}^{fast} and \hat{i}_c^{fast} are quite different and the correlation coefficient between \hat{i}_{pcc}^{fast} and \hat{i}_c^{fast} (calculated as 0.275) is low. Therefore, in this situation, $|\hat{V}_{u-pcc}^B|$ is theoretically matched with $|\hat{V}_{u-pcc}^{sup}|$ instead of $|\hat{V}_{u-pcc}^{IEC}|$ when the harmonic impedances are estimated correctly. The calculated background harmonics shown in Figure 16 (b) indicate that $|\hat{V}_{u-pcc}^{sup}|$ is exactly matched with $|\hat{V}_{u-pcc}^B|$. In comparison, obvious differences exist between $|\hat{V}_{u-pcc}^{IEC}|$ and $|\hat{V}_{u-pcc}^B|$. Hence, only $|\hat{V}_{u-pcc}^{sup}|$ can be used to validate the calculated Z_u and Z_c . Otherwise, once $|\hat{V}_{u-pcc}^{IEC}|$ is chosen to be matched with $|\hat{V}_{u-pcc}^B|$, wrong conclusion will be drawn that the calculated harmonic impedances are with large errors.

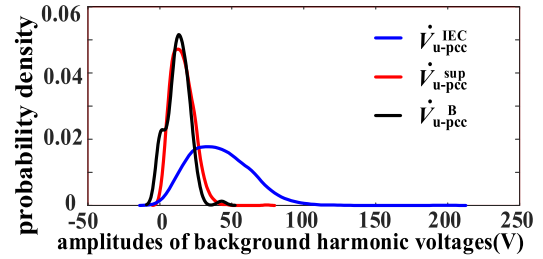


FIGURE 17. Probability density of background harmonic voltages.

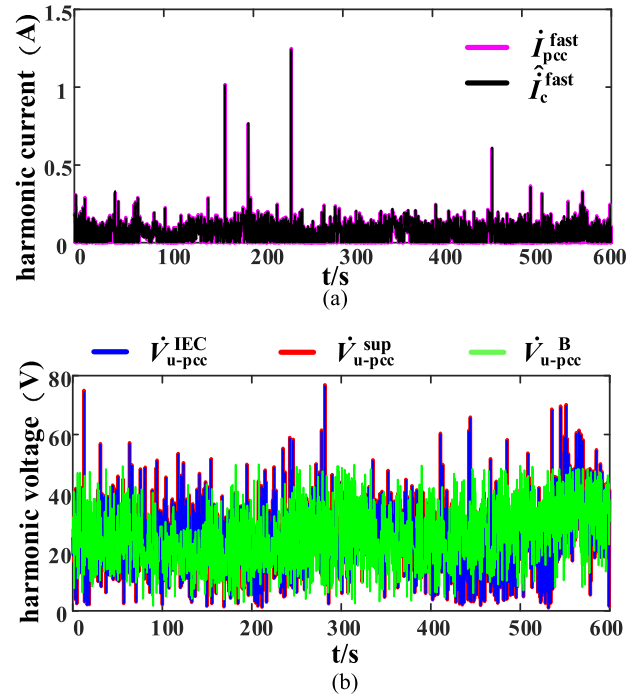


FIGURE 18. The 9th harmonic waveforms of the photovoltaic farm. (a) Extracted \hat{i}_{pcc}^{fast} and estimated \hat{i}_c^{fast} . (b) Calculated and measured background harmonics.

Moreover, the probability density curve of $|\hat{V}_{u-pcc}^{sup}|$ is close to $|\hat{V}_{u-pcc}^B|$, while $|\hat{V}_{u-pcc}^{IEC}|$ is quite different from $|\hat{V}_{u-pcc}^B|$ as shown in Figure 17. Thus, it can be further concluded that for customer in model B, if $|Z_c|$ is not much larger than $|Z_u|$, only $|\hat{V}_{u-pcc}^{sup}|$ can be chosen to judge the correctness of the calculated harmonic impedances.

2) THE 9TH HARMONICS

Because the currents \hat{i}_c^{fast} estimated by ICA is consistent with the extracted \hat{i}_{pcc}^{fast} as shown in Figure 18, and the correlation coefficient between \hat{i}_{pcc}^{fast} and \hat{i}_c^{fast} (calculated as 0.998) is larger than 0.9, $|Z_c| \gg |Z_u|$ can be determined. In this situation, theoretically, the calculated Z_u can be validated by matching either $|\hat{V}_{u-pcc}^{sup}|$ or $|\hat{V}_{u-pcc}^{IEC}|$ with $|\hat{V}_{u-pcc}^B|$. In fact, Figure 18 shows that both $|\hat{V}_{u-pcc}^{sup}|$ and $|\hat{V}_{u-pcc}^{IEC}|$ are exactly matched with $|\hat{V}_{u-pcc}^B|$. Thus, it can be concluded that the calculated Z_u is with high accuracy.

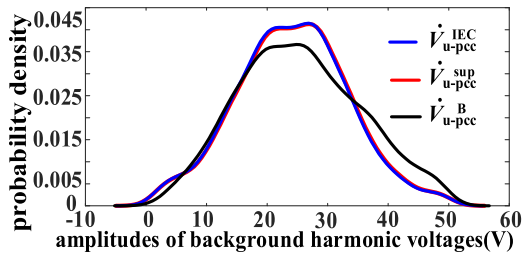


FIGURE 19. Probability density of background harmonic voltages.

What's more, the probability density curves of $|\dot{V}_{u-pcc}^{\text{sup}}|$ and $|\dot{V}_{u-pcc}^{\text{IEC}}|$ are highly similar with $|\dot{V}_{u-pcc}^{\text{B}}|$ as shown in Figure 19. Thus, the above conclusions are further validated.

C. DISCUSSION

On the basis of the above practical verification, the outcomes of the research in this paper are analyzed as follows:

1) The method based on background harmonic matching can effectively verify the validity of the harmonic impedance. Yet, misjudgment does exist in the validating process.

2) Before validating the calculated harmonic impedance, the amplitude relationship between Z_c and Z_u should be judged.

3) If $|Z_c|$ is not much larger than $|Z_u|$, the customer must be classified in model A or model B. For model A, the measured background harmonic voltage must be matched with the voltage calculated by the IEC method. Yet, for model B, the background harmonic voltage must be calculated by the superposition index while validating.

4) If $|Z_c| \gg |Z_u|$, the measured background harmonic voltage can be matched with the voltage calculated by either IEC method or the by the superposition index no matter what the model the customer belongs to.

As a result, the effectiveness the proposed framework has been verified.

V. CONCLUSION

This paper focuses on the validation of the calculated harmonic impedance and proposes a framework to validate it. The main contributions are as follows:

1) The blank research about the validation of the calculated harmonic impedance has been consummated.

2) By analyzing the properties of the IEC method and the superposition index, find that the two methods cannot be chosen arbitrarily to validate the calculated harmonic impedance. Otherwise, some misjudgments may occur.

3) The customers are divided into two models according to the way how they are out of operation, and the differences between the IEC method and the superposition index are analyzed in detail to distinguish their applicability for these two models.

4) To accurately validate the calculated harmonic impedance, an effective framework is proposed without affecting the normal operation of the power system. The simulation and the field case study have demonstrated the effectiveness and reliability of the proposed framework.

REFERENCES

- [1] W. A. Omran, H. S. K. El-Goharey, M. Kazerani, and M. M. A. Salama, "Identification and measurement of harmonic pollution for radial and non-radial systems," *IEEE Trans. Power Del.*, vol. 24, no. 3, pp. 1642–1650, Jul. 2009.
- [2] H. Hu, Y. Shao, L. Tang, J. Ma, Z. He, and S. Gao, "Overview of harmonic and resonance in railway electrification systems," *IEEE Trans. Ind. Appl.*, vol. 54, no. 5, pp. 5227–5245, Sep./Oct. 2018.
- [3] F. Safargholi, K. Malekian, and W. Schufft, "On the dominant harmonic source identification—Part I: Review of methods," *IEEE Trans. Power Del.*, vol. 33, no. 3, pp. 1268–1277, Jun. 2018.
- [4] F. Xu, H. Yang, M. Ye, Y. Liu, and J. Hui, "Classification for power quality short duration disturbances based on generalized S-transform," *Proc. CSEE*, vol. 32, no. 4, pp. 77–84 and 15, Feb. 2012.
- [5] D. Borkowski, "A new method for noninvasive measurement of grid harmonic impedance with data selection," *Int. Trans. Elect. Energy Syst.*, vol. 25, no. 12, pp. 3772–3791, Dec. 2015.
- [6] F. Karimzadeh, S. Esmaili, and S. H. Hosseini, "A novel method for noninvasive estimation of utility harmonic impedance based on complex independent component analysis," *IEEE Trans. Power Del.*, vol. 30, no. 4, pp. 1843–1852, Aug. 2015.
- [7] D. Borkowski, A. Wetula, and A. Bien, "New method for noninvasive measurement of utility harmonic impedance," in *Proc. IEEE Power Energy Soc. Gen. Meeting*, Jul. 2012, pp. 1–8.
- [8] A. Zebardast and H. Mokhtari, "New method for assessing the utility harmonic impedance based on fuzzy logic," *IET Gener., Transmiss. Distrib.*, vol. 11, no. 10, pp. 2448–2456, Jul. 2017.
- [9] J. Hui, W. Freitas, J. C. M. Vieira, H. Yang, and Y. Liu, "Utility harmonic impedance measurement based on data selection," *IEEE Trans. Power Del.*, vol. 27, no. 4, pp. 2193–2202, Oct. 2012.
- [10] Y. Wang, W. Xu, J. Yong, and K.-L. Chen, "Estimating harmonic impact of individual loads using harmonic phasor data," *Int. Trans. Elect. Energy Syst.*, vol. 27, no. 10, p. e2384, Oct. 2017.
- [11] J. Hui, H. Yang, S. Lin, and M. Ye, "Assessing utility harmonic impedance based on the covariance characteristic of random vectors," *IEEE Trans. Power Del.*, vol. 25, no. 3, pp. 1778–1786, Jul. 2010.
- [12] X. Zhao and H. Yang, "A new method to calculate the utility harmonic impedance based on FastICA," *IEEE Trans. Power Del.*, vol. 31, no. 1, pp. 381–388, Feb. 2016.
- [13] F. Karimzadeh, S. Hossein Hosseini, and S. Esmaili, "Method for determining utility and consumer harmonic contributions based on complex independent component analysis," *IET Gener., Transmiss. Distrib.*, vol. 10, no. 2, pp. 526–534, Feb. 2016.
- [14] H. Hu, P. Pan, Y. Song, and Z. He, "A novel controlled frequency band impedance measurement approach for single-phase railway traction power system," *IEEE Trans. Ind. Electron.*, vol. 67, no. 1, pp. 244–253, Jan. 2020.
- [15] Q. Shu, Y. Wu, F. Xu, and H. Zheng, "Estimate utility harmonic impedance via the cor-relation of harmonic measurements in different time intervals," *IEEE Trans. Power Del.*, early access, Dec. 17, 2019, doi: 10.1109/TPWRD.2019.2960415.
- [16] W. Xu and Y. Liu, "A method for determining customer and utility harmonic contributions at the point of common coupling," *IEEE Trans. Power Del.*, vol. 15, no. 2, pp. 804–811, Apr. 2000.
- [17] T. Pfajfar, B. Blazic, and I. Papic, "Harmonic contributions evaluation with the harmonic current vector method," *IEEE Trans. Power Del.*, vol. 23, no. 1, pp. 425–433, Jan. 2008.
- [18] A. Robert, "Guide for assessing the network harmonic impedance," in *Proc. 14th Int. Conf. Exhib. Electr. Distrib. (CIRED)*, 1997, pp. 1–3.
- [19] C. Li and W. Xu, "On defining harmonic contributions at the point of common coupling," *IEEE Power Eng. Rev.*, vol. 22, no. 7, pp. 44–45, Jul. 2002.
- [20] W. Xu, X. Liu, and Y. Liu, "An investigation on the validity of power-direction method for harmonic source determination," *IEEE Trans. Power Del.*, vol. 18, no. 1, pp. 214–219, Jan. 2003.
- [21] F. Xu, H. Yang, J. Zhao, Z. Wang, and Y. Liu, "Study on constraints for harmonic source determination using active power direction," *IEEE Trans. Power Del.*, vol. 33, no. 6, pp. 2683–2692, Dec. 2018.
- [22] *Electromagnetic Compatibility (EMC), Part 3: Limits, Section 6: Assessment of Harmonic Emission Limits for the Connection of Distorting Installations to MV, HV and EHV Power Systems*, Standard IEC 61000-3-6, 2008.
- [23] T. Pfajfar, B. Blazic, and I. Papic, "Methods for estimating customer voltage harmonic emission levels," in *Proc. 13th Int. Conf. Harmon. Qual. Power*, Wollongong, NSW, Australia, Sep. 2008, pp. 1–6.



determination, and harmonic emissions assessment.

FANGWEI XU (Member, IEEE) was born in Renshou, Sichuan, China, in 1978. She received the M.S degree in electrical engineering from Chongqing University, in 2004, and the Ph.D. degree in power system and its automation from Sichuan University, Chengdu, Sichuan, in 2012. She is currently a Professor at the College of Electrical Engineering, Sichuan University, Chengdu. Her main research interests focus on power quality characteristics extraction, harmonic source



ZHIQUAN MA was born in Nanning, Guangxi, China, in 1983. He received the M.S. degree in electrical engineering from the Huazhong University, in 2008. He is currently a Senior Engineer at the State Grid Zhejiang Electric Power Research Institute, Hangzhou, Zhejiang, China. His main research interest focuses on power quality filed test.



WEI PU was born in Meishan, Sichuan, China, in 1996. She is currently pursuing the M.S degree in electrical engineering with Sichuan University, Chengdu, Sichuan. Her main research interests are power system harmonic analysis and evaluation.



JINSHUAI ZHAO (Student Member, IEEE) was born in Yibin, Sichuan, China, in 1992. He received the B.S. degree from the College of Electrical Engineering and Information Technology, Sichuan University, Chengdu, China, in 2015, where he is currently pursuing the Ph.D. degree in power system and its automation. His main research interests are power system harmonic analysis and evaluation.



WENTAO LV was born in Mudanjiang, Heilongjiang, China, in 1989. He received the M.S. degree in electrical engineering from Zhejiang University, in 2014. He is currently an Engineer at the State Grid Zhejiang Electric Power Research Institute, Hangzhou, Zhejiang, China. His main research interests focus on power electronics, power quality, FACTS, and HVDC.

...